UNIFIED A POSTERIORI ERROR ESTIMATOR FOR FINITE ELEMENT METHODS FOR THE STOKES EQUATIONS

JUNPING WANG*, YANQIU WANG†, AND XIU YE‡

Abstract. This paper is concerned with residual type a posteriori error estimators for finite element methods for the Stokes equations. In particular, the authors established a unified approach for deriving and analyzing a posteriori error estimators for velocity-pressure based finite element formulations for the Stokes equations. A general a posteriori error estimator was presented with a unified mathematical analysis for the general finite element formulation that covers conforming, nonconforming, and discontinuous Galerkin methods as examples. The key behind the mathematical analysis is the use of a lifting operator from discontinuous finite element spaces to continuous ones for which all the terms involving jumps at interior edges disappear.

Key words. A posteriori error estimate, finite element methods, Stokes equations

AMS subject classifications. Primary, 65N15, 65N30, 76D07; Secondary, 35B45, 35J50

1. Introduction. A posteriori error estimator refers to a computable formula that offers a measure for judging the reliability and efficiency of a particular numerical scheme employed for approximating the solution of partial differential equations or alike. With a mathematically justified a posteriori error estimator, one would be able to generate a mesh that is tailored at reducing computational errors at places of great need. This process is commonly known as *adaptive mesh refinement* which has become a useful and important tool in today's scientific and engineering computing. The goal of this paper is to offer a systematic framework for developing and analyzing a posteriori error estimators for finite element methods for model Stokes equations.

This paper is concerned with residual type a posteriori error estimators. In other words, the computable formula for judging the efficiency and reliability of numerical schemes shall be given by functions of residuals. Along this avenue, several fine results have been developed for finite element methods for the Stokes equations. For conforming finite element methods, some a posteriori error estimators have been derived for mini-elements by Verfurth [21] and Bank-Welfert [4]. Ainsworth-Oden [3] and Nobile [18] have considered more general conforming finite elements in their study. For nonconforming finite elements, a posteriori error estimation for the Crouzeix-Raviart element [8] has been developed by several researchers such as Verfurth [22], Dari-Durán-Padra [9] and Doerfler-Ainsworth [10]. Carstensen, Gudi, and Jensen [5] proposed and analyzed an a posteriori error estimator for discontinuous Galerkin methods by using a stress-velocity-pressure formulation for the Stokes equations. Kay and Silvester [16] established a posteriori error estimation for the stabilized finite element formulation. The recovery based a posteriori error estimate for the Stokes equations is investigated in [12].

*Division of Mathematical Sciences, National Science Foundation, Arlington, VA 22230 (jwang@nsf.gov). The research of Wang was supported by the NSF IR/D program, while working at the Foundation. However, any opinion, finding, and conclusions or recommendations expressed in this material are those of the author and do not necessarily reflect the views of the National Science Foundation.

†Department of Mathematics, Oklahoma State University, Stillwater, OK 74075 (yqwang@math.okstate.edu).

‡Department of Mathematics, University of Arkansas at Little Rock, Little Rock, AR 72204 (xxye@ualr.edu).This research was supported in part by National Science Foundation Grant DMS-0813571

In both [9] and [10], the analysis for their a posteriori error estimators was based on a Helmholtz decomposition for decomposing the Crouzeix-Raviart element into two parts: an exactly divergence-free part and the second as its orthogonal complement. While the Helmholtz decomposition offers an applaudable approach for analyzing the efficiency and reliability of a posteriori error estimators for the Stokes equations, the method has difficulty in being extended to finite element approximations arising from discontinuous Galerkin methods. The main difficulty comes from the fact that the approximate velocity field from the discontinuous finite element methods is not divergence-free in the classical sense. Therefore, other analytical techniques have been developed for discontinuous finite elements; but most of them requires special and unnecessary properties about the finite element mesh. For example, Houston, Schötzau and Wihler [14] have developed an a posteriori error analysis for the discontinuous $Q_k - Q_{k-1}$ element on partitions consisting of parallelograms only.

In this paper, we establish a unified approach for deriving and analyzing a posteriori error estimators of residual type for velocity-pressure based formulations of the Stokes equations. In particular, we shall develop a general finite element formulation that covers conforming, non-conforming, and discontinuous Galerkin methods as examples. Then, a general a posteriori error estimator shall be presented with a unified mathematical analysis. The key behind the analysis is the use of a lifting operator from discontinuous finite element spaces to continuous ones for which all the terms involving jumps at interior edges disappear. A similar lifting operator was employed by Karakashian and Pascal [15] for analyzing a posteriori error estimates for a discontinuous Galerkin approximation to second order elliptic equations.

The paper is organized as follows. In Section 2, a model Stokes problem and some notations are introduced. In Section 3, we shall first present a general finite element formulation for the Stokes equations, and then illustrate how most existing conforming, nonconforming, and discontinuous Galerkin methods be represented by the general framework. In Section 4, we establish an analytical tool for analyzing the general a posteriori error estimator of residual type. Finally in Section 5, we present some numerical results to confirm the theory developed in previous sections.

2. Preliminaries and notations. Let Ω be an open bounded domain in $\mathbb{R}^d, d = 2, 3$. Denote by $\partial\Omega$ the boundary of Ω. The model problem seeks a velocity function $\mathbf{u}$ and a pressure function p satisfying

$$-\Delta\mathbf{u} + \nabla p = \mathbf{f} \quad \text{in } \Omega, \tag{2.1}$$

$$\nabla \cdot \mathbf{u} = 0 \quad \text{in } \Omega, \tag{2.2}$$

$$\mathbf{u} = 0 \quad \text{on } \partial\Omega, \tag{2.3}$$

where Δ, ∇, and $\nabla\cdot$ denote the Laplacian, gradient, and divergence operators, respectively, and $\mathbf{f}$ is the external volumetric force acting on the fluid.

For simplicity, the algorithm and its analysis will be presented for the model Stokes problem (2.1)-(2.3) only in two-dimensional spaces (i.e.; $d = 2$) with polygonal domains. An extension to the Stokes problem in three dimensions can be made formally for general polyhedral domains.

For any given polygon $D \subseteq \Omega$, we use the standard definition of Sobolev spaces $H^s(D)$ with $s \geq 0$ (e.g., see [1, 6] for details). The associated inner product, norm, and seminorms in $H^s(D)$ are denoted by $(\cdot,\cdot)_{s,D}$, $\|\cdot\|_{s,D}$, and $|\cdot|_{r,D}, 0 \leq r \leq s$, respectively. When $s = 0$, $H^0(D)$ coincides with the space of square integrable functions $L^2(D)$. In this case, the subscript s is suppressed from the notation of norm, semi-norm, and

inner products. Furthermore, the subscript D is also suppressed when $D = \Omega$. Denote by $L_0^2(D)$ the subspace of $L^2(D)$ consisting of functions with mean value zero.

The above definition/notation can easily be extended to vector-valued and matrix-valued functions. The norm, semi-norms, and inner-product for such functions shall follow the same naming convention. In addition, all these definitions can be transferred from a polygonal domain D to an edge e, a domain with lower dimension. Similar notation system will be employed. For example, $\|\cdot\|_{s,e}$ and $\|\cdot\|_e$ would denote the norm in $H^s(e)$ and $L^2(e)$ etc.

Throughout the paper, we follow the convention that a bold Latin letter denotes a vector. Let $\mathbf{u} = [u_i]_{1\le i\le 2}$, $\mathbf{v} = [v_i]_{1\le i\le 2}$ be two vectors, and $\sigma = [\sigma_{ij}]_{1\le i,j\le 2}$, $\tau = [\tau_{ij}]_{1\le i,j\le 2}$ be two matrices, define

$$\nabla\mathbf{v} = \begin{pmatrix} \frac{\partial v_1}{\partial x} & \frac{\partial v_1}{\partial y} \\ \frac{\partial v_2}{\partial x} & \frac{\partial v_2}{\partial y} \end{pmatrix}, \qquad \nabla\cdot\mathbf{v} = \frac{\partial v_1}{\partial x} + \frac{\partial v_2}{\partial y},$$

$$\mathbf{u}\otimes\mathbf{v} = \begin{pmatrix} u_1v_1 & u_1v_2 \\ u_2v_1 & u_2v_2 \end{pmatrix}, \qquad \sigma : \tau = \sum_{i,j=1}^{2} \sigma_{ij}\tau_{ij},$$

$$\mathbf{v}\cdot\sigma = \begin{pmatrix} \sigma_{11}v_1 + \sigma_{12}v_2 \\ \sigma_{21}v_1 + \sigma_{22}v_2 \end{pmatrix}, \qquad \mathbf{v}\cdot\sigma\cdot\mathbf{u} = \sum_{i,j=1}^{2} \sigma_{ij}u_iv_j.$$

It is not hard to see that

$$\sigma : (\mathbf{u}\otimes\mathbf{v}) = \mathbf{v}\cdot\sigma\cdot\mathbf{u}.$$

Let $\mathcal{T}_h$ be a geometrically conformal triangulation of the domain Ω; i.e., the intersection of any two triangles in $\mathcal{T}_h$ is either empty, a common vertex, or a common edge. Denote by h_T the diameter of triangle $T \in \mathcal{T}_h$, and h the maximum of all h_T. We assume that $\mathcal{T}_h$ is shape regular in the sense that for each $T \in \mathcal{T}_h$, the ratio between h_T and the diameter of the inscribed circle is bounded from above. The shape regularity of $\mathcal{T}_h$ ensures a validity of the inverse inequality for finite element functions. In addition, shape regularity allows one to apply the routine scaling arguments in finite element analysis.

Let us introduce two finite dimensional spaces V_s and P_t as follows:

$$V_s = \{\mathbf{v} \in V :\ \mathbf{v}|_T \in [P_s(T)]^2,\ \text{for all } T \in \mathcal{T}_h\},$$
$$P_t = \{q \in L_0^2(\Omega) :\ q|_T \in P_t(T),\ \text{for all } T \in \mathcal{T}_h\},$$

where $V = [L^2(\Omega)]^2$ or $[H_0^1(\Omega)]^2$, s and t are non-negative integers, and $P_k(T)$ is the set of polynomials of degree no more than k on T. A finite element method usually seeks discrete velocity and pressure approximations in some subspaces $V_h \subseteq V_s$ and $Q_h \subseteq Q_t$. Certain continuity condition may be imposed on V_h and Q_h, depending on the type of finite elements. For a posteriori error estimates only, V_h and Q_h are not required to satisfy the discrete inf-sup condition. However, we do need to make the following assumption

$$\{\mathbf{v} \in [H_0^1(\Omega)]^2 :\ \mathbf{v}|_T \in [P_1(T)]^2,\ \text{for all } T \in \mathcal{T}_h\} \subseteq V_h, \tag{2.4}$$

in the analysis of the a posteriori error estimates. For a finite element partition $\mathcal{T}_h$, with triangles only, (2.4) is satisfied as long as k, order of the polynomials, is no less

than 1. Therefore, the assumption (2.4) is reasonable and examples that satisfy it will be given later.

Denote by $\mathcal{E}_h$ the set of all edges in $\mathcal{T}_h$, and denote by $\mathcal{E}_h^0 := \mathcal{E}_h \backslash \partial\Omega$ the collection of all interior edges. Next, we define the average and jump on edges for scalar-valued function q, vector-valued function $\mathbf{w}$, and matrix-valued function τ, respectively. For any interior edge $e \in \mathcal{E}_h^0$, let T_1, T_2 be two triangles sharing e and $\mathbf{n}_1$ and $\mathbf{n}_2$ be the unit outward normal vectors on e, associated with T_1 and T_2, respectively. Define the average $\{\cdot\}$ and jump $[\![\cdot]\!]$ on e by

$$\begin{aligned}
\{q\} &= \frac{1}{2}(q|_{T_1} + q|_{T_2}), & [\![q]\!] &= q|_{T_1}\mathbf{n}_1 + q|_{T_2}\mathbf{n}_2,\\
\{\mathbf{w}\} &= \frac{1}{2}(\mathbf{w}|_{T_1} + \mathbf{w}|_{T_2}), & [\![\mathbf{w}]\!] &= \mathbf{w}|_{T_1}\cdot\mathbf{n}_1 + \mathbf{w}|_{T_2}\cdot\mathbf{n}_2,\\
\{\tau\} &= \frac{1}{2}(\tau|_{T_1} + \tau|_{T_2}), & [\![\tau]\!] &= \mathbf{n}_1\cdot\tau|_{T_1} + \mathbf{n}_2\cdot\tau|_{T_2}.
\end{aligned}$$

We also define a matrix-valued jump $[\cdot]$ for $\mathbf{w}$ on e by

$$[\mathbf{w}] = \mathbf{w}|_{T_1}\otimes\mathbf{n}_1 + \mathbf{w}|_{T_2}\otimes\mathbf{n}_2.$$

If e is a boundary edge, the above definitions need to be adjusted accordingly so that both the average and the jump are equal to the one-sided values on e. That is,

$$\begin{aligned}
&\{q\} = q|_e, && \{\mathbf{w}\} = \mathbf{w}|_e, && \{\tau\} = \tau|_e,\\
&[\![q]\!] = q|_e\mathbf{n}, && [\![\mathbf{w}]\!] = \mathbf{w}|_e\cdot\mathbf{n}, && [\![\tau]\!] = \mathbf{n}\cdot\tau|_e,\\
&[\mathbf{w}] = \mathbf{w}|_e\otimes\mathbf{n},
\end{aligned}$$

where $\mathbf{n}$ is the unit outward normal of Ω.

Let q, $\mathbf{v}$ and τ be scalar-, vector-, and matrix-valued functions that are regular enough to make all involving terms well-defined, then the following identities are standard [2]:

$$\sum_{T\in\mathcal{T}_h}\int_{\partial T} q\,\mathbf{v}\cdot\mathbf{n}\,ds = \sum_{e\in\mathcal{E}_h^0}\int_e [\![q]\!]\cdot\{\mathbf{v}\}\,ds + \sum_{e\in\mathcal{E}_h}\int_e \{q\}[\![\mathbf{v}]\!]\,ds, \tag{2.5}$$

$$\sum_{T\in\mathcal{T}_h}\int_{\partial T} \mathbf{n}\cdot\tau\cdot\mathbf{v}\,ds = \sum_{e\in\mathcal{E}_h^0}\int_e [\![\tau]\!]\cdot\{\mathbf{v}\}\,ds + \sum_{e\in\mathcal{E}_h}\int_e \{\tau\} : [\mathbf{v}]\,ds. \tag{2.6}$$

3. Finite element formulation. We first derive a general weak formulation for the Stokes equations that covers a set of existing numerical methods including discontinuous Galerkin, conforming finite elements, and some nonconforming finite element schemes. To this end, let $\mathbf{v}$ and $\mathbf{w}$ be vector-valued functions, and we introduce the following notation

$$\begin{aligned}
(\mathbf{v},\ \mathbf{w})_{\mathcal{T}_h} &:= \sum_{K\in\mathcal{T}_h}\int_K \mathbf{v}\cdot\mathbf{w}\,dx,\\
(\mathbf{v},\ \mathbf{w})_{\mathcal{E}_h} &:= \sum_{e\in\mathcal{E}_h}\int_e \mathbf{v}\cdot\mathbf{w}\,ds.
\end{aligned}$$

Testing the momentum equation (2.1) by $\mathbf{v}\in V_h$ yields

$$-(\Delta\mathbf{u},\ \mathbf{v}) + (\nabla p,\ \mathbf{v}) = (\mathbf{f},\ \mathbf{v}). \tag{3.1}$$

Next, using integration by parts, Equation (2.6) and the fact that $[\![\nabla \mathbf{u}]\!] = 0$ on all $e \in \mathcal{E}_h^0$, we have

$$\begin{aligned} -(\Delta \mathbf{u},\ \mathbf{v}) &= (\nabla \mathbf{u},\ \nabla \mathbf{v})_{\mathcal{T}_h} - \sum_{K \in \mathcal{T}_h} \int_{\partial K} \mathbf{n} \cdot \nabla \mathbf{u} \cdot \mathbf{v}\, ds \\ &= (\nabla \mathbf{u},\ \nabla \mathbf{v})_{\mathcal{T}_h} - (\{\nabla \mathbf{u}\},\ [\mathbf{v}])_{\mathcal{E}_h}. \end{aligned}$$

Analogously, since $[\![p]\!] = 0$ on all $e \in \mathcal{E}_h^0$, then by using Equation (2.5) we arrive at

$$\begin{aligned} (\nabla p,\ \mathbf{v}) &= -(\nabla \cdot \mathbf{v},\ p)_{\mathcal{T}_h} + \sum_{K \in \mathcal{T}_h} \int_{\partial K} \mathbf{v} \cdot \mathbf{n}\, p\, ds \\ &= -(\nabla \cdot \mathbf{v},\ p)_{\mathcal{T}_h} + (\{p\},\ [\![\mathbf{v}]\!])_{\mathcal{E}_h}. \end{aligned}$$

Thus, (3.1) can be rewritten as

$$(\nabla \mathbf{u},\ \nabla \mathbf{v})_{\mathcal{T}_h} - (\{\nabla \mathbf{u}\},\ [\mathbf{v}])_{\mathcal{E}_h} - (\nabla \cdot \mathbf{v},\ p)_{\mathcal{T}_h} + (\{p\},\ [\![\mathbf{v}]\!])_{\mathcal{E}_h} = (\mathbf{f},\ \mathbf{v}). \tag{3.2}$$

The mass conservation equation (2.2) can be tested by using any $q \in Q_h$, yielding

$$(\nabla \cdot \mathbf{u},\ q)_{\mathcal{T}_h} = 0. \tag{3.3}$$

In order to derive a general weak formulation, we introduce the following bilinear forms:

$$\begin{aligned} a(\mathbf{u}, \mathbf{v}) &:= (\nabla \mathbf{u}, \nabla \mathbf{v})_{\mathcal{T}_h} \\ &\quad -\gamma \Big((\{\nabla \mathbf{u}\},\ [\mathbf{v}])_{\mathcal{E}_h} + \delta (\{\nabla \mathbf{v}\},\ [\mathbf{u}])_{\mathcal{E}_h} - \alpha (h_e^{-1} [\mathbf{u}],\ [\mathbf{v}])_{\mathcal{E}_h} \Big), \qquad (3.4) \\ b(\mathbf{v}, p) &:= -(\nabla \cdot \mathbf{v},\ p)_{\mathcal{T}_h} + \gamma ([\![\mathbf{v}]\!], \{p\})_{\mathcal{E}_h}, \qquad (3.5) \end{aligned}$$

where $\gamma = 0$ or 1, $\delta = 1$, -1 or 0, and $\alpha \geq 0$ are parameters with various values. The general weak formulation for the Stokes equations is then given as follows:

Algorithm G: Find $(\mathbf{u}_h; p_h) \in V_h \times Q_h$ such that

$$a(\mathbf{u}_h, \mathbf{v}) + b(\mathbf{v}, p_h) = (\mathbf{f}, \mathbf{v}), \tag{3.6}$$

$$b(\mathbf{u}_h,\ q) = 0 \tag{3.7}$$

for all $(\mathbf{v}; q) \in V_h \times Q_h$.

When $\gamma = 1$, it is not hard to see that system (3.6)-(3.7) is consistent with the system (3.2)-(3.3), as the exact solution of the Stokes problem satisfies $[\![\mathbf{u}]\!] = 0$ and $[\mathbf{u}] = 0$ on all $e \in \mathcal{E}_h$. When $\gamma = 0$, these two systems are in general not consistent. It should be pointed out that by choosing different values of γ and the spaces V_h and Q_h, **Algorithm G** represents different types of finite element formulations. For illustrative purpose, we shall list three most important examples; all of which satisfy the assumption (2.4) on V_h.

Example 1: Discontinuous Galerkin. Set $\gamma = 1$ and

$$\begin{aligned} V_h &\subseteq \{\mathbf{v} \in [L^2(\Omega)]^2 :\ \mathbf{v}|_T \in [P_s(T)]^2,\ \text{for all } T \in \mathcal{T}_h\}, \\ Q_h &\subseteq \{q \in L_0^2(\Omega) :\ q|_T \in P_t(T),\ \text{for all } T \in \mathcal{T}_h\}. \end{aligned}$$

When $\delta = 1$, the corresponding formulation is symmetric. One example of such a discontinuous Galerkin formulation was discussed in [25], where V_h, Q_h are chosen to be $H(div)$ conforming elements and the well-known inf-sup condition was inherited to be valid.

Example 2: Conforming finite element method. Set $\gamma = 1$ and

$$V_h \subseteq \{\mathbf{v} \in [H_0^1(\Omega)]^2 : \ \mathbf{v}|_T \in [P_s(T)]^2, \text{ for all } T \in \mathcal{T}_h\},$$
$$Q_h \subseteq \{q \in L_0^2(\Omega) : \ q|_T \in P_t(T), \text{ for all } T \in \mathcal{T}_h\}.$$

By the continuity requirement on V_h, we easily see that the two bilinear forms are simplified to

$$a(\mathbf{v}, \mathbf{w}) = (\nabla \mathbf{v}, \nabla \mathbf{w}),$$
$$b(\mathbf{v}, q) = -(\nabla \cdot \mathbf{v}, \ q).$$

The conforming finite element scheme is one of the most well-studied formulations for the Stokes problems. Later in the section for numerical experiments, we shall consider one such element, namely, the Taylor-Hood element [13].

Example 3: Nonconforming finite element method. Set $\gamma = 0$ and chose a finite element space V_h such that $V_h \nsubseteq [H_0^1(\Omega)]^2$. This gives some nonconforming finite element methods, depending on the selection of V_h and Q_h. In this paper, we only consider nonconforming finite elements which satisfies the following condition:

Assumption (H) $\qquad (\{\nabla \mathbf{u} - pI\}, \ [\mathbf{v}])_{\mathcal{E}_h} = 0 \qquad$ for all $\mathbf{u}, \mathbf{v} \in V_h, \ p \in Q_h,$

where I is the 2×2 identity matrix. It is not hard to see that the Crouzeix-Raviart type nonconforming elements [8, 11, 7] satisfy this assumption, because by its definition, $\{\nabla \mathbf{u} - pI\}$ is a polynomial one degree lower than $[\mathbf{v}]$ and $[\mathbf{v}]$ vanishes at all Gaussian points on each edge $e \in \mathcal{E}_h$.

The goal of this manuscript is to provide a tool that can be employed to analyze a posteriori error estimators for the unified formulation (3.6)-(3.7). To this end, we first derive an orthogonality property of the error between the exact solution and its finite element approximation:

$$\mathbf{e} = \mathbf{u} - \mathbf{u}_h, \quad \epsilon = p - p_h.$$

By subtracting (3.6) from (3.2) and using $(\{p_h\}, \ [\![\mathbf{v}]\!])_{\mathcal{E}_h} = (\{p_h I\}, \ [\mathbf{v}])_{\mathcal{E}_h}$, we have

$$(\nabla \mathbf{e}, \nabla \mathbf{v})_{\mathcal{T}_h} - (\{\nabla \mathbf{e}\}, \ [\mathbf{v}])_{\mathcal{E}_h} + \gamma\Big(\delta(\{\nabla \mathbf{v}\}, \ [\mathbf{u}_h])_{\mathcal{E}_h} - \alpha(h_e^{-1}[\mathbf{u}_h], \ [\mathbf{v}])_{\mathcal{E}_h}\Big)$$
$$- (\nabla \cdot \mathbf{v}, \epsilon)_{\mathcal{T}_h} + (\{\epsilon\}, \ [\![\mathbf{v}]\!])_{\mathcal{E}_h} - (1-\gamma)(\{\nabla \mathbf{u}_h - p_h I\}, \ [\mathbf{v}])_{\mathcal{E}_h} = 0.$$

Note that for all of the above-mentioned discontinuous Galerkin, conforming and nonconforming cases, we must have

$$(1-\gamma)(\{\nabla \mathbf{u}_h - p_h I\}, \ [\mathbf{v}])_{\mathcal{E}_h} = 0. \tag{3.8}$$

In fact, (3.8) follows from $\gamma = 1$ for the discontinuous Galerkin and the conforming cases, and from Assumption (H) for the nonconforming case. Combining this and the fact that $[\mathbf{u}] = 0$ on all edges, the above equation can be rewritten as

$$(\nabla \mathbf{e}, \nabla \mathbf{v})_{\mathcal{T}_h} - (\{\nabla \mathbf{e}\},\ [\mathbf{v}])_{\mathcal{E}_h} - \gamma\Big(\delta(\{\nabla \mathbf{v}\},\ [\mathbf{e}])_{\mathcal{E}_h} - \alpha(h_e^{-1}[\mathbf{e}],\ [\mathbf{v}])_{\mathcal{E}_h}\Big) - (\nabla \cdot \mathbf{v}, \epsilon)_{\mathcal{T}_h} + (\{\epsilon\},\ [\![\mathbf{v}]\!])_{\mathcal{E}_h} = 0. \tag{3.9}$$

Moreover, if $\mathbf{v} \in V_h \cap [H_0^1(\Omega)]^2$, then (3.9) becomes

$$(\nabla \mathbf{e}, \nabla \mathbf{v})_{\mathcal{T}_h} + \gamma\delta(\{\nabla \mathbf{v}\},\ [\mathbf{u}_h])_{\mathcal{E}_h} - (\nabla \cdot \mathbf{v}, \epsilon)_{\mathcal{T}_h} = 0. \tag{3.10}$$

Next, we introduce a norm $|\!|\!| \cdot |\!|\!|$ for the space $[H_0^1(\Omega)]^2 + V_h$ as follows

$$|\!|\!|\mathbf{v}|\!|\!|^2 = \sum_{T \in \mathcal{T}_h} |\mathbf{v}|_{1,T}^2 + \sum_{e \in \mathcal{E}_h} h_e^{-1} \|[\mathbf{v}]\|_e^2. \tag{3.11}$$

For a well-crafted numerical scheme, we usually expect to have an a priori error estimate like the following

$$|\!|\!|\mathbf{e}|\!|\!| + \|\epsilon\| \le C h^{k+1} \left(|\mathbf{u}|_{k+1} + |p|_k\right), \tag{3.12}$$

where C is a positive constant and k is determined by the order of the corresponding finite elements and the regularity of the exact solution $(\mathbf{u}; p)$. For some elements, the a priori error estimate (3.12) may have variations on the right-hand side, but this does not affect our analysis to be presented. A priori error estimation like (3.12) is well known for conforming finite element methods, for which $|\!|\!|\mathbf{v}|\!|\!| = |\mathbf{v}|_1$. Such an estimate is also known for some discontinuous Galerkin formulations; e.g., see [24, 25] for an approach with $H(div)$-elements. For nonconforming finite elements, such as the Crouzeix-Raviart type elements, similar error estimates hold true due to the fact that the jump term, $[\mathbf{u}_h]$, vanishes at all Gaussian points on the edge e. In fact, for any interior edge e shared by two elements T_1 and T_2, let $\bar{\mathbf{e}}$ be the average value of $\mathbf{e}$ on edge e. Since $[\mathbf{e}] = -[\mathbf{u}_h]$ vanishes at all Gaussian points on the edge e, then $\bar{\mathbf{e}}$ has the same value when the trace of $\mathbf{e}$ was taken from either T_1 or T_2. Hence,

$$\begin{aligned} h_e^{-1}\|[\mathbf{e}]\|_e^2 &= h_e^{-1}\|[\mathbf{e} - \bar{\mathbf{e}}]\|_e^2 \\ &\le 2h_e^{-1} \sum_{T_1, T_2} \|\mathbf{e} - \bar{\mathbf{e}}\|_{e \cap \partial T_i}^2 \\ &\le C \sum_{T_1, T_2} |\mathbf{e}|_{1,T_i}^2. \end{aligned}$$

Consequently, we have

$$\sum_{e \in \mathcal{E}_h} h_e^{-1}\|[\mathbf{e}]\|_e^2 \le C \sum_{T \in \mathcal{T}_h} |\mathbf{e}|_{1,T}^2.$$

Therefore, $|\!|\!|\mathbf{e}|\!|\!|$ is in the same order as $\sum_{T \in \mathcal{T}_h} |\mathbf{e}|_{1,T}^2$ for the Crouzeix-Raviart type elements. The analysis here shows that the norm $|\!|\!| \cdot |\!|\!|$ as defined in (3.11) is a reasonable one to use in the a priori and later the a posteriori error estimates for the unified formulation (3.6)-(3.7).

4. A posteriori error estimation. The goal of this section is to derive an a posteriori error estimation for the **Algorithm G** by using a unified framework. For simplicity of notation, we shall use "$\lesssim$" to denote "less than or equal to up to a constant independent of the mesh size, variables, or other parameters appearing in the inequality". To this end, define

$$\mathbf{J}_1(\nabla \mathbf{u}_h - p_h I) = \begin{cases} [\![\nabla \mathbf{u}_h - p_h I]\!] & \text{on } e \in \mathcal{E}_h^0, \\ 0 & \text{on boundary edges,} \end{cases}$$

and

$$\mathbf{J}_2(\mathbf{u}_h) = \begin{cases} [\mathbf{u}_h] & \text{on } e \in \mathcal{E}_h^0, \\ 2\mathbf{u}_h \otimes \mathbf{n} & \text{on boundary edges.} \end{cases}$$

Our residual-based global error estimator is given by

$$\eta^2 = \sum_{T \in \mathcal{T}_h} \eta_T^2, \tag{4.1}$$

where

$$\begin{aligned} \eta_T^2 =& h_T^2 \|\mathbf{f}_h + \Delta \mathbf{u}_h - \nabla p_h\|_T^2 + \|\nabla \cdot \mathbf{u}_h\|_T^2 \\ &+ \frac{1}{2} \sum_{e \in \mathcal{E}_h} \int_e \left(h_e \mathbf{J}_1(\nabla \mathbf{u}_h - p_h I)^2 + h_e^{-1} \mathbf{J}_2(\mathbf{u}_h)^2 \right) ds, \end{aligned}$$

with h_e being the length of edge e, and $\mathbf{f}_h$ the L^2 projection of the load function $\mathbf{f}$ onto V_h. It is also convenient to introduce an oscillation quantity for the load function $\mathbf{f}$ on $\mathcal{T}_h$ as follows

$$\mathrm{osc}(\mathbf{f}) = \left(\sum_{T \in \mathcal{T}_h} h_T^2 \|\mathbf{f} - \mathbf{f}_h\|_T^2 \right)^{1/2}.$$

Our ultimate goal is to establish the following result.

THEOREM 4.1. *Let $(\mathbf{u}; p)$ be the solution of (2.1)-(2.2), and $(\mathbf{u}_h; p_h)$ be its finite element approximation arising from (3.6)-(3.7). Then, one has*

$$\left(\sum_{T \in \mathcal{T}_h} \|\nabla(\mathbf{u} - \mathbf{u}_h)\|_T^2 \right)^{1/2} + \|p - p_h\| \lesssim \eta + \mathrm{osc}(\mathbf{f}) \tag{4.2}$$

and

$$\eta \lesssim \left(\sum_{T \in \mathcal{T}_h} \|\nabla(\mathbf{u} - \mathbf{u}_h)\|_T^2 \right)^{1/2} + \|p - p_h\| + \mathrm{osc}(\mathbf{f}). \tag{4.3}$$

For convenience, the relation (4.2) is referred to as a reliability estimate and (4.3) as an efficiency estimate.

4.1. A lifting operator and some technical estimates. Define $H^1(\mathcal{T}_h) = \prod_{T \in \mathcal{T}_h} H^1(T)$ and $S_k = \prod_{T \in \mathcal{T}_h} P_k(T)$. For any triangle $T \in \mathcal{T}_h$, denote by $\mathcal{T}(T)$ the set of all triangles in $\mathcal{T}_h$ having a nonempty intersect with T, including T itself. Denote by $\mathcal{E}(T)$ the set of all edges in $\mathcal{E}_h$ having a nonempty intersection with T,

including all three edges of T. Similarly, for any point x in Ω, denote by $\mathcal{E}(x)$ the set of all edges that pass through x. Note that $\mathcal{E}(x)$ is nonempty only when x lies on $\mathcal{E}_h$. Let e be an edge of triangle T. For any $v \in S_k$, let us define a lifting operator

$$L_k : v \to L_k(v) \in S_k \cap H_0^1(\Omega) \tag{4.4}$$

that lifts a discontinuous piecewise polynomial to a continuous piecewise polynomial with vanishing boundary trace as follows. Let $G_k(T)$ be the set of all Lagrangian nodal points for $P_k(T)$. At all internal Lagrangian nodal points $x_j \in G_k(T)$, we set $L_k(v)(x_j) = v(x_j)$. At boundary Lagrangian points $x_j \in G_k(T) \cap \partial T$, we let $L_k(v)(x_j)$ be either a trace of v from any side or a prescribed weighted average of all possible traces. At global Lagrangian points $x_j \in \partial T \cap \partial\Omega$, we set $L_k(v)(x_j) = 0$.

Note that for any function $g \in H^1(T)$ the following estimate holds:

$$\|g\|_e^2 \lesssim h_T^{-1}\|g\|_T^2 + h_T\|\nabla g\|_T^2. \tag{4.5}$$

LEMMA 4.2. *For any $v \in S_k$, $k \geq 1$, the lifting operator L_k as defined in (4.4) satisfies the following estimate:*

$$\|v - L_k(v)\|_T^2 + h_T^2\|\nabla(v - L_k(v))\|_T^2 \lesssim \sum_{e \in \mathcal{E}(T)} h_e\|[\![v]\!]\|_e^2 \qquad \forall T \in \mathcal{T}_h. \tag{4.6}$$

Proof. The proof follows from a routine scaling argument and the fact that all norms on finite dimensional spaces are equivalent. To this end, we observe that

$$\|v - L_k(v)\|_T^2 + h_T^2\|\nabla(v - L_k(v))\|_T^2 \lesssim h_T^2 \sum_{x_j \in G_k(T)} |(v - L_k(v))(x_j)|^2,$$

where $G_k(T)$ is the set of all Lagrangian nodal points for $P_k(T)$. For simplicity, let $L_k(v)$ be defined by taking a random one-sided trace on the boundary Lagrangian points. It follows from the definition of L_k that $v - L_k(v)$ vanishes at all internal Lagrangian points in T. At Lagrangian points on ∂T, there are two possibilities: (1) x_j is in the interior of an edge e; (2) x_j is a vertex of T. In the first case, we see that $|(v - L_k(v))(x_j)|$ is either 0 or $|[\![v]\!]_e(x_j)|$, where $[\![v]\!]_e$ denotes the jump on e. In the second case, we can use the triangle inequality to traverse through all edges $e \in \mathcal{E}(x_j)$ and to obtain

$$|(v - L_k(v))(x_j)| \leq \sum_{e \in \mathcal{E}(x_j)} |[\![v]\!]_e(x_j)|.$$

The above analysis, together with the shape regularity of $\mathcal{T}_h$, implies that

$$\sum_{x_j \in G_k(T)} |(v - L_k(v))(x_j)|^2 \lesssim \sum_{e \in \mathcal{E}(T)} \sum_{x_j \in G_k(e)} |[\![v]\!]_e(x_j)|^2,$$

where $G_k(e)$ was used to denote the corresponding Lagrangian points on edge e. Then, using the routine scaling argument on edges, inequality (4.6) follows immediately. ∎

The following is another result that turns out to be very useful in the forthcoming analysis.

LEMMA 4.3. *For any $v \in H^1(\mathcal{T}_h)$, there exists a $v_I \in S_k \cap H_0^1(\Omega)$, $k \geq 1$, satisfying*

$$\|v - v_I\|_T^2 + h_T^2 \|\nabla(v - v_I)\|_T^2 \lesssim \sum_{T' \in \mathcal{T}(T)} h_{T'}^2 \|\nabla v\|_{T'}^2 + \sum_{e \in \mathcal{E}(T)} h_e \|[\![v]\!]\|_e^2 \qquad \forall T \in \mathcal{T}_h. \tag{4.7}$$

Proof. First of all, there exists a piecewise constant $v_0 \in S_k$ (e.g., the cell average of v) such that

$$\|v - v_0\|_T^2 + h_T^2 \|\nabla(v - v_0)\|_T^2 \lesssim h_T^2 \|\nabla v\|_T^2 \qquad \forall T \in \mathcal{T}_h. \tag{4.8}$$

Furthermore, by the approximation property, inequality (4.5) and the shape regularity of $\mathcal{T}_h$, we have for each $e \in \mathcal{E}_h^0$

$$\begin{aligned} h_e \|[\![v_0]\!]\|_e^2 &= h_e \int_e \left| v_0|_{T_1} \mathbf{n}_1 + v_0|_{T_2} \mathbf{n}_2 \right|^2 ds \\ &\leq h_e \int_e \left| (v_0 - v)|_{T_1} \mathbf{n}_1 \right|^2 ds + h_e \int_e \left| (v_0 - v)|_{T_2} \mathbf{n}_2 \right|^2 ds + h_e \|[\![v]\!]\|_e^2 \\ &\lesssim h_{T_1}^2 \|\nabla v\|_{T_1}^2 + h_{T_2}^2 \|\nabla v\|_{T_2}^2 + h_e \|[\![v]\!]\|_e^2, \end{aligned} \tag{4.9}$$

where T_1 and T_2 are the two triangles sharing e as a common edge. On boundary edges, similar result can obviously be obtained without any difficulty.

Since $v_0 \in S_k$ with $k = 1$, according to Lemma 4.2, one may lift v_0 to a continuous piecewise linear function $L_1(v_0) \in S_1 \cap H_0^1(\Omega)$ which satisfies (4.6). By taking $v_I = L_1(v_0)$, we obtain from the usual triangle inequality, (4.8), and (4.9) that

$$\begin{aligned} \|v - v_I\|_T^2 + h_T^2 \|\nabla(v - v_I)\|_T^2 \leq & \|v - v_0\|_T^2 + h_T^2 \|\nabla(v - v_0)\|_T^2 \\ & + \|v_0 - L_1(v_0)\|_T^2 + h_T^2 \|\nabla(v_0 - L_1(v_0))\|_T^2 \\ \lesssim & h_T^2 \|\nabla v\|_T^2 + \sum_{e \in \mathcal{E}(T)} h_e \|[\![v_0]\!]\|_e^2 \\ \lesssim & \sum_{T' \in \mathcal{T}(T)} h_{T'}^2 \|\nabla v\|_{T'}^2 + \sum_{e \in \mathcal{E}(T)} h_e \|[\![v]\!]\|_e^2, \end{aligned}$$

which completes the proof. ∎

4.2. Reliability estimate. We first establish an estimate for the pressure error in terms of the a priori error estimator and the velocity error. The result can be stated as follows.

LEMMA 4.4. *Let $(\mathbf{u}; p)$ be the solution of (2.1)-(2.2) and $(\mathbf{u}_h; p_h)$ be its finite element approximation arising from (3.6)-(3.7). Then, we have*

$$\|p - p_h\| \lesssim \eta + \mathrm{osc}(\mathbf{f}) + \left(\sum_{T \in \mathcal{T}_h} \|\nabla(\mathbf{u} - \mathbf{u}_h)\|_T^2 \right)^{1/2}. \tag{4.10}$$

Proof. Let $\mathbf{v} \in [H_0^1(\Omega)]^2$ and $\mathbf{v}_I \in V_h \cap [H_0^1(\Omega)]^2$ be an interpolation of $\mathbf{v}$ such that both components satisfy (4.7). Observe that such an interpolation $\mathbf{v}_I$ is possible if V_h satisfies the assumption (2.4). Note that $[\![\mathbf{v}]\!] = 0$ on every edge since $\mathbf{v} \in [H_0^1(\Omega)]^2$.

Let $\mathbf{e} = \mathbf{u} - \mathbf{u}_h$ and $\epsilon = p - p_h$ be the error for velocity and pressure approximations, respectively. Using integration by parts, (2.6), (3.10), (4.5), (4.7), and the fact that both $\mathbf{v}$ and $\mathbf{v}_I$ are continuous across each interior, we arrive at

$$\begin{aligned}
(\nabla\cdot\mathbf{v},\ \epsilon) &= (\nabla\cdot(\mathbf{v}-\mathbf{v}_I),\ \epsilon) + (\nabla\cdot\mathbf{v}_I,\ \epsilon)\\
&= (\nabla\cdot(\mathbf{v}-\mathbf{v}_I),\ \epsilon) + (\nabla\mathbf{e},\ \nabla\mathbf{v}_I)_{\mathcal{T}_h} + \gamma\delta(\{\nabla\mathbf{v}_I\},\ [\mathbf{e}])_{\mathcal{E}_h}\\
&= (\nabla(\mathbf{v}-\mathbf{v}_I),\ \epsilon I - \nabla\mathbf{e})_{\mathcal{T}_h} + (\nabla\mathbf{e},\ \nabla\mathbf{v})_{\mathcal{T}_h} + \gamma\delta(\{\nabla\mathbf{v}_I\},\ [\mathbf{e}])_{\mathcal{E}_h}\\
&= -(\mathbf{f}+\Delta\mathbf{u}_h - \nabla p_h,\ \mathbf{v}-\mathbf{v}_I)_{\mathcal{T}_h} + (\{\mathbf{v}-\mathbf{v}_I\},\ [\![\nabla\mathbf{u}_h - p_h I]\!])_{\mathcal{E}_h^0}\\
&\qquad -\gamma\delta(\{\nabla\mathbf{v}_I\},\ [\mathbf{u}_h])_{\mathcal{E}_h} + (\nabla\mathbf{e},\ \nabla\mathbf{v})_{\mathcal{T}_h}\\
&\lesssim \|\mathbf{v}\|_1\Big(\big(\sum_{T\in\mathcal{T}_h} h_T^2\|\mathbf{f}+\Delta\mathbf{u}_h-\nabla p_h\|_T^2\big)^{1/2} + \big(\sum_{e\in\mathcal{E}_h^0} h_e\|[\![\nabla\mathbf{u}_h - p_h I]\!]\|_e^2\big)^{1/2}\\
&\qquad +\big(\sum_{e\in\mathcal{E}_h} h_e^{-1}\|[\mathbf{u}_h]\|_e^2\big)^{1/2} + \big(\sum_{T\in\mathcal{T}_h}\|\nabla\mathbf{e}\|_T^2\big)^{1/2}\Big),
\end{aligned}$$

which, together with the following inf-sup condition

$$\|p-p_h\| \lesssim \sup_{\mathbf{v}\in[H_0^1(\Omega)]^2} \frac{(\nabla\cdot\mathbf{v},\, p-p_h)}{\|\mathbf{v}\|_1} \tag{4.11}$$

yields the required estimate (4.10). □

The next result is concerned with an estimate for the velocity approximation, which can be stated as follow.

THEOREM 4.5. *Let $(\mathbf{u};p)$ and $(\mathbf{u}_h;p_h)$ be the solutions of (2.1)-(2.2) and (3.6)-(3.7). Then one has the following global reliability estimate:*

$$\left(\sum_{T\in\mathcal{T}_h}\|\nabla(\mathbf{u}-\mathbf{u}_h)\|_T^2\right)^{1/2} \lesssim \eta + \mathrm{osc}(\mathbf{f}). \tag{4.12}$$

Substituting (4.12) into (4.10) yields the following estimate for the pressure approximation:

$$\|p-p_h\| \lesssim \eta + \mathrm{osc}(\mathbf{f}). \tag{4.13}$$

Thus, it follows from the definition of $|||\cdot|||$ that

$$|||\mathbf{e}||| + \|\epsilon\| \lesssim \eta + \mathrm{osc}(\mathbf{f}).$$

Proof. Let $\mathbf{e}_I \in V_h \cap [H_0^1(\Omega)]^2$ be an interpolation of $\mathbf{e}$ satisfying (4.7). Again, such a choice of $\mathbf{e}_I$ is possible because V_h was assumed to satisfy (2.4). Observe that $[\![\mathbf{e}]\!] = -[\![\mathbf{u}_h]\!]$. Thus, it follows from (4.7) and the mesh regularity that

$$\|\mathbf{e}-\mathbf{e}_I\|_T^2 + h_T^2\|\nabla(\mathbf{e}-\mathbf{e}_I)\|_T^2 \lesssim h_T^2\left(\sum_{T'\in\mathcal{T}(T)}\|\nabla\mathbf{e}\|_{T'}^2 + \sum_{e\in\mathcal{E}(T)} h_e^{-1}\|\mathbf{J}_2(\mathbf{u}_h)\|_e^2\right). \tag{4.14}$$

Using (3.10), integration by parts, (2.6), and the fact that $\mathbf{e}_I$, $\mathbf{u}$, $\nabla\mathbf{u}$, p are continuous across all interior edges, we obtain

$$\begin{aligned}
(\nabla\mathbf{e},\ \nabla\mathbf{e})_{\mathcal{T}_h} &= (\nabla\mathbf{e},\ \nabla(\mathbf{e}-\mathbf{e}_I))_{\mathcal{T}_h} + (\nabla\mathbf{e},\ \nabla\mathbf{e}_I)_{\mathcal{T}_h} \\
&= (\nabla\mathbf{e},\ \nabla(\mathbf{e}-\mathbf{e}_I))_{\mathcal{T}_h} + (\nabla\cdot\mathbf{e}_I,\ \epsilon) - \gamma\delta(\{\nabla\mathbf{e}_I\},\ [\mathbf{e}])_{\mathcal{E}_h} \\
&= (\nabla(\mathbf{e}-\mathbf{e}_I),\ \nabla\mathbf{e}-\epsilon I)_{\mathcal{T}_h} + (\nabla\cdot\mathbf{e},\ \epsilon)_{\mathcal{T}_h} - \gamma\delta(\{\nabla\mathbf{e}_I\},\ [\mathbf{e}])_{\mathcal{E}_h} \\
&= (\mathbf{f}+\Delta\mathbf{u}_h-\nabla p_h,\ \mathbf{e}-\mathbf{e}_I)_{\mathcal{T}_h} + (\nabla\cdot\mathbf{e},\ \epsilon)_{\mathcal{T}_h} - \gamma\delta(\{\nabla\mathbf{e}_I\},\ [\mathbf{e}])_{\mathcal{E}_h} \\
&\qquad -(\{\mathbf{e}-\mathbf{e}_I\},\ [\![\nabla\mathbf{u}_h - p_h I]\!])_{\mathcal{E}_h^0} - (\{\nabla\mathbf{e}-\epsilon I\},\ [\mathbf{u}_h])_{\mathcal{E}_h} \\
&= (\mathbf{f}+\Delta\mathbf{u}_h-\nabla p_h,\ \mathbf{e}-\mathbf{e}_I)_{\mathcal{T}_h} + (\nabla\cdot\mathbf{e},\ \epsilon)_{\mathcal{T}_h} - \gamma\delta(\{\nabla\mathbf{e}_I\},\ [\mathbf{e}])_{\mathcal{E}_h} \\
&\qquad -(\{\mathbf{e}-\mathbf{e}_I\},\ [\![\nabla\mathbf{u}_h - p_h I]\!])_{\mathcal{E}_h^0} - (\{\nabla\mathbf{e}-\epsilon I\},\ [\mathbf{u}_h-\chi])_{\mathcal{E}_h} \\
&= I_1 + I_2 + I_3 + I_4 + I_5; \qquad (4.15)
\end{aligned}$$

where $\chi = L_k(\mathbf{u}_h) \in V_h \cap [H_0^1(\Omega)]^2$ is a continuous interpolation of $\mathbf{u}_h$ such that (4.6) is satisfied, and I_j represents the corresponding term from the previous equation. The first term I_1 can be estimated by using the inequality (4.14) as follows

$$\begin{aligned}
|I_1| &\le \left(\sum_{T\in\mathcal{T}_h} h_T^2\|\mathbf{f}+\Delta\mathbf{u}_h-\nabla p_h\|_T^2\right)^{\frac{1}{2}} \left(\sum_{T\in\mathcal{T}_h} h_T^{-2}\|\mathbf{e}-\mathbf{e}_I\|_T^2\right)^{\frac{1}{2}} \\
&\lesssim \left(\sum_{T\in\mathcal{T}_h} h_T^2\|\mathbf{f}+\Delta\mathbf{u}_h-\nabla p_h\|_T^2\right)^{\frac{1}{2}} \left(\sum_{T\in\mathcal{T}_h}\|\nabla\mathbf{e}\|_T^2 + \sum_{e\in\mathcal{E}_h} h_e^{-1}\|\mathbf{J}_2(\mathbf{u}_h)\|_e^2\right)^{\frac{1}{2}} \\
&\lesssim (\eta+\mathrm{osc}(\mathbf{f}))\left(\eta + \left(\sum_{T\in\mathcal{T}_h}\|\nabla\mathbf{e}\|_T^2\right)^{1/2}\right). \qquad (4.16)
\end{aligned}$$

The term I_2 can be handled by using (4.10) and the fact that $\nabla\cdot\mathbf{e} = -\nabla\cdot\mathbf{u}_h$ as follows

$$\begin{aligned}
|I_2| &\le \left(\sum_{T\in\mathcal{T}_h}\|\nabla\cdot\mathbf{u}_h\|_T^2\right)^{1/2}\|p-p_h\| \\
&\lesssim \eta\left(\eta + \mathrm{osc}(\mathbf{f}) + \left(\sum_{T\in\mathcal{T}_h}\|\nabla\mathbf{e}\|_T^2\right)^{1/2}\right). \qquad (4.17)
\end{aligned}$$

Using $[\mathbf{e}] = -[\mathbf{u}_h]$ and the estimate (4.14), the term I_3 can be bounded as follows

$$\begin{aligned}
|I_3| &\le |\gamma\delta|\left(\sum_{e\in\mathcal{E}_h} h_e\|\nabla\mathbf{e}_I\|_e^2\right)^{\frac{1}{2}} \left(\sum_{e\in\mathcal{E}_h} h_e^{-1}\|[\mathbf{u}_h]\|_e^2\right)^{\frac{1}{2}} \\
&\lesssim \left(\sum_{T\in\mathcal{T}_h}\|\nabla\mathbf{e}_I\|_T^2\right)^{\frac{1}{2}} \left(\sum_{e\in\mathcal{E}_h} h_e^{-1}\|[\mathbf{u}_h]\|_e^2\right)^{\frac{1}{2}} \\
&\lesssim \left(\sum_{T\in\mathcal{T}_h}\|\nabla\mathbf{e}\|_T^2 + \sum_{e\in\mathcal{E}_h} h_e^{-1}\|[\mathbf{u}_h]\|_e^2\right)^{\frac{1}{2}} \left(\sum_{e\in\mathcal{E}_h} h_e^{-1}\|[\mathbf{u}_h]\|_e^2\right)^{\frac{1}{2}} \\
&\lesssim \left(\left(\sum_{T\in\mathcal{T}_h}\|\nabla\mathbf{e}\|_T^2\right)^{\frac{1}{2}} + \eta\right)\eta. \qquad (4.18)
\end{aligned}$$

The same argument can be applied to provide an estimate for the term I_4:

$$|I_4| \leq \left(\left(\sum_{T\in\mathcal{T}_h} \|\nabla \mathbf{e}\|_T^2 \right)^{\frac{1}{2}} + \eta \right) \eta. \tag{4.19}$$

As to I_5, we first use (3.9) to obtain

$$\begin{aligned}
-I_5 =&(\{\nabla \mathbf{e} - \epsilon I\},\ [\mathbf{u}_h - \chi])_{\mathcal{E}_h} \\
=&(\{\nabla \mathbf{e}\},\ [\mathbf{u}_h - \chi])_{\mathcal{E}_h} - (\{\epsilon\},\ [\![\mathbf{u}_h - \chi]\!])_{\mathcal{E}_h} \\
=&(\nabla \mathbf{e},\ \nabla(\mathbf{u}_h - \chi))_{\mathcal{T}_h} - \gamma\delta(\{\nabla(\mathbf{u}_h - \chi)\},\ [\mathbf{e}])_{\mathcal{E}_h} + \gamma\alpha(h_e^{-1}[\mathbf{u}_h - \chi],\ [\mathbf{e}])_{\mathcal{E}_h} \\
&\quad - (\nabla \cdot (\mathbf{u}_h - \chi),\ \epsilon)_{\mathcal{T}_h} \\
=&(\nabla \mathbf{e},\ \nabla(\mathbf{u}_h - \chi))_{\mathcal{T}_h} - \gamma\delta(\{\nabla(\mathbf{u}_h - \chi)\},\ [\mathbf{e}])_{\mathcal{E}_h} - \gamma\alpha(h_e^{-1}[\mathbf{u}_h],\ [\mathbf{u}_h])_{\mathcal{E}_h} \\
&\quad - (\nabla \cdot (\mathbf{u}_h - \chi),\ \epsilon)_{\mathcal{T}_h} \\
=&J_1 + J_2 + J_3 + J_4.
\end{aligned}$$

Recall that $\chi = L_k(\mathbf{u}_h)$ is a lift of $\mathbf{u}_h$ so that the estimate (4.6) holds true. It follows from (4.6) that

$$|J_1| \leq \eta \left(\sum_{T\in\mathcal{T}_h} \|\nabla \mathbf{e}\|_T^2 \right)^{\frac{1}{2}}$$

Next, we use $[\mathbf{e}] = -[\mathbf{u}_h]$ to obtain

$$|J_2| \leq |\gamma\delta| \sum_{e\in\mathcal{E}_h} \|\nabla(\mathbf{u}_h - L_k(\mathbf{u}_h))\|_e \|[\mathbf{u}_h]\|_e,$$

which, with the help of (4.5) and (4.6), can be bounded by

$$|J_2| \lesssim \eta^2.$$

It is obvious that $|J_3| \lesssim \eta^2$, and it follows from (4.10) and (4.6) that

$$|J_4| \lesssim \eta \left(\eta + \mathrm{osc}(\mathbf{f}) + (\nabla \mathbf{e},\ \nabla \mathbf{e})_{\mathcal{T}_h}^{\frac{1}{2}} \right).$$

Collecting all the estimates for J_s yields

$$|I_5| \lesssim \eta \left(\eta + \mathrm{osc}(\mathbf{f}) + (\nabla \mathbf{e},\ \nabla \mathbf{e})_{\mathcal{T}_h}^{\frac{1}{2}} \right). \tag{4.20}$$

Now we substitute all the estimates for I_s into (4.15) to obtain

$$\begin{aligned}
(\nabla \mathbf{e},\ \nabla \mathbf{e})_{\mathcal{T}_h} &\lesssim (\eta + \mathrm{osc}(\mathbf{f})) \left(\eta + \mathrm{osc}(\mathbf{f}) + \left(\sum_{T\in\mathcal{T}_h} \|\nabla \mathbf{e}\|_T^2 \right)^{1/2} \right) \\
&\leq \frac{3}{2}(\eta + \mathrm{osc}(\mathbf{f}))^2 + \frac{1}{2}(\nabla \mathbf{e},\ \nabla \mathbf{e})_{\mathcal{T}_h}.
\end{aligned}$$

This completes the proof of (4.12). □

4.3. Efficiency. We first define two bubble functions, which are widely used in a posteriori error estimations [23].

For each triangle $T \in \mathcal{T}_h$, denote by ϕ_T the following bubble function

$$\phi_T = \begin{cases} 27\,\lambda_1\lambda_2\lambda_3 & \text{in } T, \\ 0 & \text{in } \Omega\backslash T, \end{cases}$$

where λ_i, $i = 1, 2, 3$ are barycentric coordinates on T. It is clear that $\phi_T \in H_0^1(\Omega)$ and satisfies the following properties [23]:

- For any polynomial q with degree at most m, there exist positive constants c_m and C_m, depending only on m, such that

$$c_m\|q\|_T^2 \le \int_T q^2\phi_T\,dx \le \|q\|_T^2, \tag{4.21}$$

$$\|\nabla(q\phi_T)\|_T \le C_m h_T^{-1}\|q\|_T. \tag{4.22}$$

For each $e \in \mathcal{E}_h^0$, we can analogously define an edge bubble function ϕ_e. Let T_1 and T_2 be two triangles sharing the edge e. To this end, denote by $\omega_e = T_1 \cup T_2$ the union of the elements T_1 and T_2. Assume that in T_i, $i = 1, 2$, the barycentric coordinates associated with the two ends of e are $\lambda_1^{T_i}$ and $\lambda_2^{T_i}$, respectively. The edge bubble function can be defined as follows

$$\phi_e = \begin{cases} 4\lambda_1^{T_1}\lambda_2^{T_1} & \text{in } T_1, \\ 4\lambda_1^{T_2}\lambda_2^{T_2} & \text{in } T_2, \\ 0 & \text{in } \Omega\backslash\omega_e. \end{cases}$$

Then $\phi_e \in H_0^1(\Omega)$ and satisfies the following properties [23]:

- For any polynomial q with degree at most m, there exist positive constants d_m, D_m and E_m, depending only on m, such that

$$d_m\|q\|_e^2 \le \int_e q^2\phi_e\,ds \le \|q\|_e^2, \tag{4.23}$$

$$\|\nabla(q\phi_e)\|_{\omega_e} \le D_m h_e^{-1/2}\|q\|_e, \tag{4.24}$$

$$\|q\phi_e\|_{\omega_e} \le E_m h_e^{1/2}\|q\|_e. \tag{4.25}$$

Then we have the following efficiency bound.

THEOREM 4.6. *Let $(\mathbf{u}; p)$ and $(\mathbf{u}_h; p_h)$ be the solutions of (2.1)-(2.2) and (3.6)-(3.7), respectively. Then for all $T \in \mathcal{T}_h$ and $e \in \mathcal{E}_h^0$, we have*

$$h_T\|\mathbf{f}_h + \Delta\mathbf{u}_h - \nabla p_h\|_T \lesssim \|\nabla\mathbf{e}\|_T + \|\epsilon\|_T + h_T\|\mathbf{f} - \mathbf{f}_h\|_T, \tag{4.26}$$

$$h_e^{1/2}\|\mathbf{J}_1(\nabla\mathbf{u}_h - p_h I)\|_e \lesssim h_e\|\mathbf{f} - \mathbf{f}_h\|_{\omega_e} + \left(\sum_{T\in\omega_e}\|\nabla\mathbf{e}\|_T^2\right)^{1/2} + \|\epsilon\|_{\omega_e}, \tag{4.27}$$

$$\|\nabla\cdot\mathbf{u}_h\|_T \le \|\nabla\mathbf{e}\|_T. \tag{4.28}$$

By summing the above estimates over all element $T \in \mathcal{T}_h$ and edges $e \in \mathcal{E}_h$, we obtain the following efficiency estimate:

$$\eta \lesssim |||\mathbf{e}||| + \|\epsilon\| + \mathrm{osc}(\mathbf{f}).$$

Proof. Let $\mathbf{w}_T = (\mathbf{f}_h + \Delta \mathbf{u}_h - \nabla p_h)\phi_T$. Since $\mathbf{f} = -\Delta \mathbf{u} + \nabla p$ and $\mathbf{w}_T$ vanishes on ∂T, we clearly have

$$(\mathbf{f} - \mathbf{f}_h,\ \mathbf{w}_T)_T + (\mathbf{f}_h + \Delta \mathbf{u}_h - \nabla p_h,\ \mathbf{w}_T)_T = (\nabla \mathbf{e},\ \nabla \mathbf{w}_T)_T - (\nabla \cdot \mathbf{w}_T,\ \epsilon\ )_T.$$

Then, by inequalities (4.21)-(4.22),

$$\begin{aligned}
\|\mathbf{f}_h + \Delta \mathbf{u}_h - \nabla p_h\|_T^2 &\lesssim (\mathbf{f}_h + \Delta \mathbf{u}_h - \nabla p_h,\ \mathbf{w}_T)_T \\
&= (\nabla \mathbf{e},\ \nabla \mathbf{w}_T)_T - (\nabla \cdot \mathbf{w}_T,\ \epsilon\ )_T - (\mathbf{f} - \mathbf{f}_h,\ \mathbf{w}_T)_T \\
&\lesssim \Big(\|\nabla \mathbf{e}\|_T + \|\epsilon\|_T \Big) \|\nabla \mathbf{w}_T\|_T + \|\mathbf{f} - \mathbf{f}_h\|_T \|\mathbf{w}_T\|_T \\
&\lesssim \Big(h_T^{-1} \|\nabla \mathbf{e}\|_T + h_T^{-1} \|\epsilon\|_T + \|\mathbf{f} - \mathbf{f}_h\|_T \Big) \|\mathbf{f}_h + \Delta \mathbf{u}_h - \nabla p_h\|_T.
\end{aligned}$$

This completes the proof of (4.26).

Similarly, for any $e \in \mathcal{E}_h^0$, let $\mathbf{w}_e = (\llbracket \nabla \mathbf{u}_h - p_h I \rrbracket)\phi_e$. Using integration by parts and the fact that $\mathbf{w}_e = 0$ on $\partial \omega_e$, we have

$$(\nabla \mathbf{u}_h, \nabla \mathbf{w}_e)_{\omega_e} = -\sum_{T \in \omega_e} (\Delta \mathbf{u}_h, \mathbf{w}_e)_T + \int_e \llbracket \nabla \mathbf{u}_h \rrbracket \cdot \mathbf{w}_e ds, \tag{4.29}$$

and

$$(\nabla \cdot \mathbf{w}_e,\ p_h)_{\omega_e} = -\sum_{T \in \omega_e} (\nabla p_h, \mathbf{w}_e)_T + \int_e \llbracket p_h I \rrbracket \cdot \mathbf{w}_e ds. \tag{4.30}$$

Testing (2.1) by using $\mathbf{w}_e$ over ω_e and then using integration by parts give

$$(\mathbf{f},\ \mathbf{w}_e)_{\omega_e} = (\nabla \mathbf{u}, \nabla \mathbf{w}_e)_{\omega_e} - (\nabla \cdot \mathbf{w}_e,\ p)_{\omega_e}. \tag{4.31}$$

Using the properties of ϕ_e and equations (4.29)-(4.31), we have

$$\begin{aligned}
&\|\llbracket \nabla \mathbf{u}_h - p_h I \rrbracket\|_e^2 \lesssim \int_e \llbracket \mathbf{u}_h - p_h I \rrbracket \cdot \mathbf{w}_e ds \\
&= \sum_{T \in \omega_e} \Big((\mathbf{f} - \mathbf{f}_h,\ \mathbf{w}_e)_T + (\mathbf{f}_h + \Delta \mathbf{u}_h - \nabla p_h,\ \mathbf{w}_e)_T - (\nabla \mathbf{e}, \nabla \mathbf{w}_e)_T + (\epsilon,\ \nabla \cdot \mathbf{w}_e)_T \Big) \\
&\lesssim \|\llbracket \nabla \mathbf{u}_h - p_h I \rrbracket\|_e \Big(h_e^{1/2} \|\mathbf{f} - \mathbf{f}_h\|_{\omega_e} + h_e^{1/2} \|\mathbf{f}_h + \Delta \mathbf{u}_h - \nabla p_h\|_{\omega_\mathbf{e}} \\
&\qquad + h_e^{-1/2} \Big(\sum_{T \in \omega_e} \|\nabla \mathbf{e}\|_T^2 \Big)^{1/2} + h_e^{-1/2} \|\epsilon\|_{\omega_e} \Big)
\end{aligned}$$

Combining the above with (4.26) gives (4.27).

Finally, the estimate (4.28) holds true as $\nabla \cdot \mathbf{u} = 0$ and clearly

$$\|\nabla \cdot \mathbf{u}_h\|_T = \|\nabla \cdot \mathbf{u}_h - \nabla \cdot \mathbf{u}\|_T = \|\nabla \cdot \mathbf{e}\|_T \le \|\nabla \mathbf{e}\|_T.$$

This completes the proof of the theorem. □

5. Numerical results. Some numerical results for such a posteriori error estimators have been reported in [10] for the Crouzeix-Raviart element, and in [24] for an $H(div)$ based discontinuous Galerkin formulation. In this section, we would like to present some computational results for the conforming finite element method in order to verify the theory established in previous Sections. To this end, we consider the Taylor-Hood element [13] when applied to the Stokes problem. We use the Bi-Conjugate Gradient (BICG) iterative solver for solving the resulting linear algebraic equations, with a relative $residual = 10^{-8}$ being set as a stopping criteria.

5.1. Test problems. Three problems are considered in the numerical test; all are defined on the domain of unit square $\Omega = (0,1) \times (0,1)$. Two of them have exact solutions given by:

Test Problem 1: A first Stokes problem with exact solution

$$\mathbf{u} = \begin{pmatrix} -2x^2y(x-1)^2(2y-1)(y-1) \\ xy^2(2x-1)(x-1)(y-1)^2 \end{pmatrix},$$
$$p = \sin\frac{\pi(y-x)}{2},$$

Test Problem 2: A second Stokes problem with exact solution in the polar coordinate system

$$\mathbf{u} = \begin{pmatrix} \frac{3}{2}\sqrt{r}\left(\cos\frac{\theta}{2} - \cos\frac{3\theta}{2}\right) \\ \frac{3}{2}\sqrt{r}\left(3\sin\frac{\theta}{2} - \sin\frac{3\theta}{2}\right) \end{pmatrix},$$
$$p = -6r^{-1/2}\cos\frac{\theta}{2}.$$

Observe that the solution has a corner singularity of order 0.5 at the origin $(0,0)$.

Test Problem 3: $2D$ lid driven cavity. This is a Stokes problem which describes the flow of fluid in a rectangular container driven by a uniform motion of the top lid [20]. Note that the boundary condition features a discontinuity at two top corners. The exact solution $(\mathbf{u}; p)$, if it exists, should not be sufficiently smooth so that $(\mathbf{u}; p) \in [H^1]^2 \times L^2$. However, the discrete problem is still well-posed and should provide an approximation to the actual solution.

It must be pointed out that the finite element formulation was only presented for the homogeneous Dirichlet boundary condition in the previous Sections. But the formulation can be easily extended to problems with non-homogeneous Dirichlet boundary conditions such as $\mathbf{u} = \mathbf{g}$ on $\partial\Omega$. In this case, the term $\mathbf{J}_2(\mathbf{u}_h)$ in the a posteriori error estimator needs to be modified as follows

$$\mathbf{J}_2(\mathbf{u}_h) = \begin{cases} [\mathbf{u}_h] & \text{on interior edge } e \in \mathcal{E}_h^0, \\ (\mathbf{u}_h - \mathbf{g}) \otimes \mathbf{n} & \text{on boundary edges.} \end{cases}$$

Also, in the computational implementation, we had replaced $h_T^2 \|\mathbf{f}_h + \Delta\mathbf{u}_h - \nabla p_h\|_T^2$ by $|T|\ \|\mathbf{f}_h + \Delta\mathbf{u}_h - \nabla p_h\|_T^2$, where $|T|$ stands for the area of triangle T.

5.2. Results with uniform meshes. In this experiment, we solve test problems 1 and 2 on uniform meshes and compute the asymptotic order of the error estimator η. The coarsest mesh is generated by dividing Ω into 4×4 sub-rectangles,

and then dividing each sub-rectangle into four triangles by connecting its two diagonal lines. We then use the routine uniform refinement procedure, which divides each triangle into four sub-triangles by connecting the center of its three edges, to generate several levels of fine meshes.

For test problem 1, we know theoretically that $\eta = O(h^2)$. For test problem 2, the order of η is expected to be $O(h^{0.5})$. Numerical results for these two test problems are reported in tables 5.1 and 5.2. For test problem 2, the error of pressure is not calculated since the pressure goes to infinity at the point $(0, 0)$.

TABLE 5.1
Error profiles for test problem 1 on uniform triangular meshes.

h	dofs	η	$\|\nabla(\mathbf{u} - \mathbf{u}_h)\|$	$\|\mathbf{u} - \mathbf{u}_h\|$	$\|p - p_h\|$
2^{-2}	331	1.70e-02	4.15e-03	1.10e-04	3.08e-03
2^{-3}	1235	4.94e-03	1.07e-03	1.38e-05	7.88e-04
2^{-4}	4771	1.30e-03	2.71e-04	1.70e-06	1.96e-04
2^{-5}	18755	3.33e-04	6.79e-05	2.13e-07	4.89e-05
Asym. Order $O(h^k)$, $k =$	-1.9423	1.8956	1.9796	3.0064	1.9931

TABLE 5.2
Error profiles for test problem 2 on uniform triangular meshes.

h	ndofs	η	$\|\nabla(\mathbf{u} - \mathbf{u}_h)\|$	$\|\mathbf{u} - \mathbf{u}_h\|$
2^{-2}	331	2.39e+00	4.76e-01	1.54e-02
2^{-3}	1235	1.63e+00	3.30e-01	5.83e-03
2^{-4}	4771	1.12e+00	2.33e-01	2.17e-03
2^{-5}	18755	7.97e-01	1.64e-01	8.09e-04
Asym. Order $O(h^k)$, $k =$	-1.9423	0.5295	0.5094	1.4183

5.3. Results with adaptive refinement. We perform adaptive refinements for test problems 2 and 3, which have corner singularities. Two different refinement strategies are employed in this study. The first one is based on a comparison of each error η_T with the maximum value of all the error estimators. The strategy can be described as follows:

Local Refinement by "Maximum Strategy":

1. Given a current triangular mesh, error indicators η_T on each triangle, and a threshold $\theta \in (0, 1)$ (e.g., $\theta = 0.5$). One computes the maximum error $\eta_{max} = \max \eta_T$.
2. For each triangle T, if $\eta_T \geq \theta \, \eta_{max}$, mark this triangle for refinement.
3. The actual refinement is done by the newest node bisection method [17, 19]. It has been proved that this method will not cause mesh degeneration. The only requirement is that the "newest nodes" for the coarsest mesh must be assigned carefully such that every triangle is compatibly divisible. This can be easily checked.

The second refinement strategy is based on a comparison of η_T with those for its neighbors. To explain the main idea, let $\rho > 0$ be a prescribed distance parameter

TABLE 5.3
Error profiles for test problem 2 using adaptive mesh refinements.

Strategy	Refinement times	dofs	η	$\|\nabla(\mathbf{u}-\mathbf{u}_h)\|$	$\|\mathbf{u}-\mathbf{u}_h\|$
Maximum	0	331	2.3955	0.4763	0.0154
	8	432	0.9453	0.1968	0.0029
	16	764	0.4021	0.0844	0.0012
Local	0	331	2.3955	0.4763	0.0154
	8	545	0.7596	0.1519	0.0012
	16	1117	0.2505	0.0618	0.0006

and set

$$\mathcal{T}_{\rho,T} = \{\tilde{T} :\ 0 < \|T - \tilde{T}\| \le \rho\},$$

where $\|T - \tilde{T}\|$ stands for the distance of the centers of T and $\tilde{T}$. With a given threshold $\theta > 1$, we mark a triangle T for refinement if

$$\eta_T \ge \theta\, \eta_{N(T)},$$

where $\eta_{N(T)}$ is the average of the local error indicator on all the neighboring triangles $\tilde{T} \in \mathcal{T}_{\rho,T}$. The following is such a refinement strategy that was numerically investigated in this study.

Local Refinement by "Local Strategy":

1. Given a current triangular mesh, error estimators η_T on each triangle, and a threshold $\theta > 1.0$ (e.g., $\theta = 1.5$). One computes an error indicator $\eta_{N(T)}$ as the average of the local error indicator on neighboring triangles that share a vertex or an edge with T, not including T itself.
2. For each triangle T, if $\eta_T \ge \theta\, \eta_{N(T)}$, mark this triangle for refinement.
3. The actual refinement is again done by the newest node bisection method [17, 19].

The residual estimator η and errors between the true solution and its finite element approximations for test problem 2 are reported in Table 5.3. By comparing tables 5.2 and 5.3, one clearly sees the power of adaptive refinements in numerical methods for PDEs. For example, the error in L^2 and H^1 norms are given by 6.0×10^{-4} and 6.18×10^{-2} with only 1117 degree of freedoms when the local adaptive refinement strategy was used, while the uniform partition requires more than 18755 degree of freedoms in order to reach a comparable accuracy.

The refined meshes after 0, 8, and 16 refinements are illustrated in Figures 5.1 and 5.2, which show that our residual estimator really captures the corresponding corner singularity correctly, under both refinement strategies. Furthermore, in Figures 5.3 and 5.4, we examine the relation of η, $\|\nabla(\mathbf{u}-\mathbf{u}_h)\|$, and $\|\mathbf{u}-\mathbf{u}_h\|$ with the degree of freedoms N during the process of the adaptive refinement. The plots start from the coarsest mesh and ends after 16 refinements.

For the driven cavity problem, since the exact solution may not be sufficiently as smooth as in $[H^1]^2 \times L^2$, the residual error η is not expected to decrease when the mesh is refined. Our numerical experiments show that the error indicator η_T is able to locate both corner singularities for this problem. The meshes after 0, 8, and 16 refinements are plotted in Figures 5.5 and 5.6. Readers are invited to make their own conclusions for the numerical results illustrated in this Section.

[1] R. Adams and J. Fournier, *Sobolev Spaces*, Academic press, 2003.

[2] D. Arnold, F. Brezzi, B. Cockburn and D. Marini, *Unified analysis of discontinuous Galerkin methods for elliptic problems*, SIAM J. Numer. Anal., 39 (2002), 1749-1779.

[3] M. Ainsworth and J.T. Oden, *A Posteriori Error Estimators for Stokes and Oseen's Equations*. SIAM J. Numer. Anal., 17 (1997), 228-246.

[4] R. Bank and B. Welfert *A Posteriori Error Estimates for the Stokes Problem*, SIAM J. Numer. Anal. 28, (1991), 591-623.

[5] C. Carstensen, T. Gudi, M. Jensen *A Unifying Theory of A Posteriori Control for Discontinuous Galerkin FEM*, Numerische Mathematik, 112, (2009), 363-379.

[6] P.G. Ciarlet, *The finite element method for elliptic problems*, North-Holland, Amsterdam, 1978.

[7] M. Crouzeix and R.S. Falk, *Nonconforming Finite Elements for the Stokes Problem*, Math. Comp., 52, (1989), 437-456.

[8] M. Crouzeix and P.-A. Raviart, *Conforming and nonconforming finite element methods for solving the stationary Stokes equations*, I. RAIRO Anal. Numér. 7, (1973), 33-76.

[9] E. Dari, R. G. Durán and C. Padra *Error estimators for nonconforming finite element approximations of the Stokes problem*, Math. Comp. 64, (1995) 1017-1033.

[10] W. Doerfler and M. Ainsworth, *Reliable a posteriori error control for non-conforming finite element approximation of Stokes flow*, Math. Comp. 74 (2005), 1599-1619.

[11] M. Fortin and M. Soulie, *A non-conforming piecewise quadratic finite element on triangles*, Int. J. Num. Meth. Eng. 19, (1983), 502-520.

[12] A. Hannukainen, R. Stenberg and M. Vohralik. *A unified framework for a posteriori error estimation for the Stokes problem*, Numerische Mathematik, submitted.

[13] P. Hood and C. Taylor, *A numerical solution of the Navier-Stokes equations using the finite element technique*, Comp. and Fluids, 1, (1973), 73-100.

[14] P. Houston, D. Schötzau and T. P. Wihler *Energy Norm A Posteriori Error Estimation for Mixed Discontinuous Galerkin Approximations of the Stokes Problem*, J. Sci. Comput., 22-23, (2005), 347-370.

[15] O. A. Karakashian and F. Pascal, *A posteriori error estimates for a discontinuous Galerkin approximation of second order elliptic problems*, SIAM J. Numer. Anal. 41 (2003), 2374-2399.

[16] David Kay and David Silvester *A posteriori error estimation for stabilised mixed approximations of the Stokes equations*, SIAM J. Scientific Computing 21, (1999), 1321-1336.

[17] W. F. Mitchell *Unified Multilevel Adaptive Finite Element Methods for Elliptic Problems*, Ph.D. dissertation, University of Illinois at Urbana-Champaign, 1988.

[18] F. Nobile, *A posteriori error estimates for the finite element approximation of the Stokes problem*, TICAM Report 03-13, April 2003.

[19] E. G. Sewell, *Automatic generation of triangulations for piecewise polynomial approximation*, Ph.D. dissertation, Purdue University, 1972.

[20] P.N. Shankar and M.D. Deshpande, *Fluid Mechanics in the driven cavity*, Annu. Rev. Fluid Mech., 32 (2000), 93-136.

[21] R. Verfurth, *A posteriori error estimators for the Stokes equations*, Numer. Math., 3, (1989), 309-325.

[22] R. Verfurth, *A posteriori error estimators for the Stokes equations II. Non-conforming discretizations.* Numer. Math. 60, (1991), 235-249.

[23] R. Verfurth, *A review of a posteriori error estimation and adaptive mesh-refinement techniques*. Teubner Skripten zur Numerik. B.G. Willey-Teubner, Stuttgart, 1996.

[24] J. Wang, Y. Wang, and X. Ye, *A posteriori error estimation for an interior panelty type method employing H(div) elements for the Stokes equations*, SIAM J. Scientific Computing, accepted.

[25] J. Wang and X. Ye, *New finite element methods in computational fluid dynamics by H(div) elements*, SIAM J. Numerical Analysis, 45 (2007), 1269-1286.

FIG. 5.1. *Test problem 2, maximum strategy adaptive refinement. Meshes after* 0, 8, *and* 16 *refinements.*

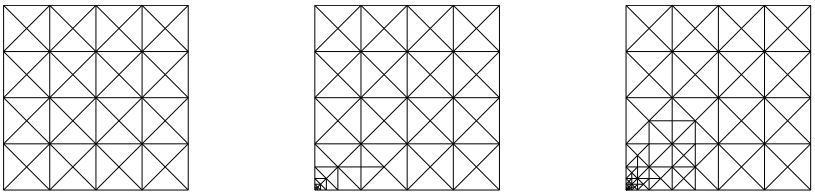

FIG. 5.2. *Test problem 2, local strategy adaptive refinement. Meshes after* 0, 8, *and* 16 *refinements.*

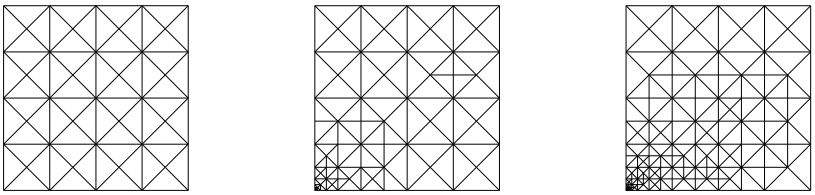

FIG. 5.3. *Test problem 2, maximum strategy adaptive refinement. Plot of* η, $\|\nabla(\mathbf{u}-\mathbf{u}_h)\|$ *and* $\|\mathbf{u}-\mathbf{u}_h\|$, *versus the degrees of freedom* N.

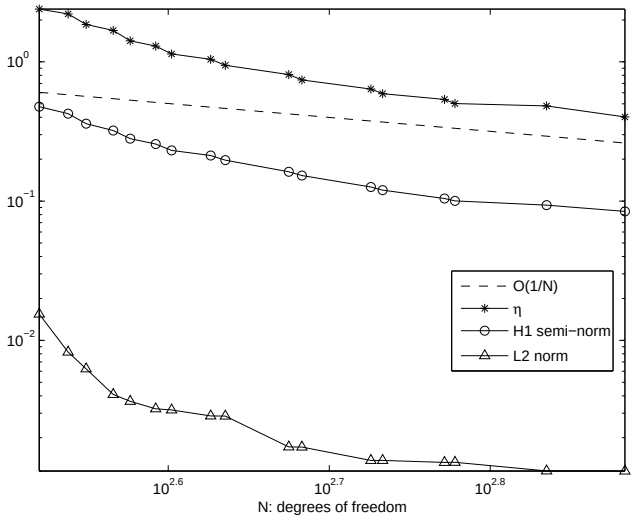

FIG. 5.4. *Test problem 2, local strategy adaptive refinement. Plot of* η, $\|\nabla(\mathbf{u}-\mathbf{u}_h)\|$ *and* $\|\mathbf{u}-\mathbf{u}_h\|$, *versus the degrees of freedom* N.

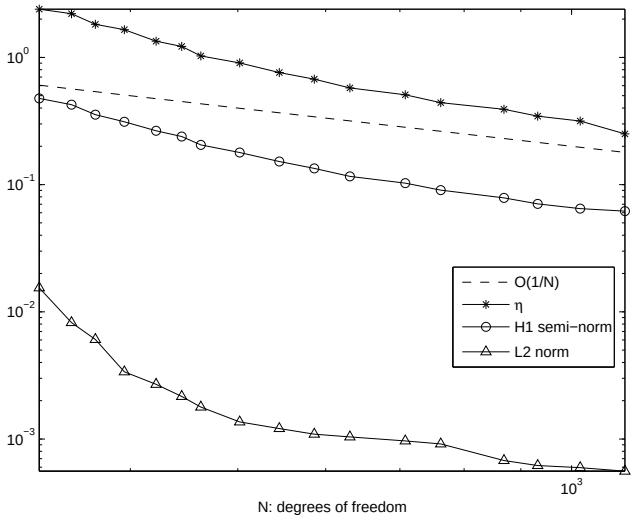

FIG. 5.5. *Test problem 3, maximum strategy adaptive refinement. Meshes after* 0, 8, *and* 16 *refinements.*

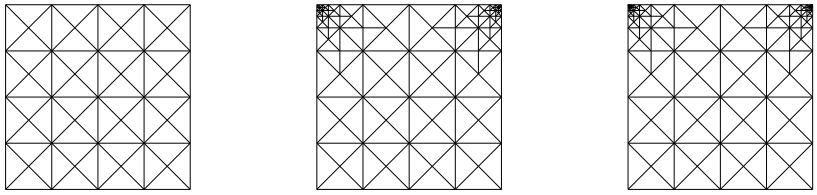

FIG. 5.6. *Test problem 3, local strategy adaptive refinement. Meshes after* 0, 8, *and* 16 *refinements.*